The Impact of Boreal Forest Fire on Climate Warming

J. T. Randerson, *et al.*

Science **314**, 1130 (2006);
DOI: 10.1126/science.1132075

The Impact of Boreal Forest Fire on Climate Warming

J. T. Randerson,[1]* H. Liu,[2] M. G. Flanner,[1] S. D. Chambers,[3] Y. Jin,[1] P. G. Hess,[4] G. Pfister,[4] M. C. Mack,[5] K. K. Treseder,[1] L. R. Welp,[6] F. S. Chapin,[7] J. W. Harden,[8] M. L. Goulden,[1] E. Lyons,[1] J. C. Neff[9] E. A. G. Schuur,[5] C. S. Zender[1]

We report measurements and analysis of a boreal forest fire, integrating the effects of greenhouse gases, aerosols, black carbon deposition on snow and sea ice, and postfire changes in surface albedo. The net effect of all agents was to increase radiative forcing during the first year (34 ± 31 Watts per square meter of burned area), but to decrease radiative forcing when averaged over an 80-year fire cycle (−2.3 ± 2.2 Watts per square meter) because multidecadal increases in surface albedo had a larger impact than fire-emitted greenhouse gases. This result implies that future increases in boreal fire may not accelerate climate warming.

Arctic and boreal regions are warming rapidly, with multiple consequences for northern ecosystems and global climate (*1*). In boreal ecosystems, future increases in air temperature may lengthen the fire season and increase the probability of fires, leading some to hypothesize a positive feedback between warming, fire activity, carbon loss, and future climate change (*2*, *3*). Although CO_2 and other greenhouse gases emitted by fire contribute to climate warming, understanding the net effect of a changing fire regime on climate is challenging because of the multiple ways by which fires influence atmospheric composition and the land surface. Emissions of aerosols, for example, can lead to either warming or cooling at a regional scale, depending on factors such as aerosol composition and the underlying albedo of both the Earth's surface and clouds (*4*). Subsequent deposition of black carbon aerosols on glaciers, snow, sea ice, and the Greenland ice sheet may reduce surface albedo (*5*), causing both atmospheric heating (*6*) and enhanced surface melting. Within a burn perimeter, combined changes in ecosystem structure and species composition after fire cause net radiation and sensible heat fluxes to decline substantially (*7*, *8*). These changes in the local surface energy budget persist for decades and are probably regionally variable. Concurrently, accumulation of carbon in organic soils and vegetation during intermediate successional stages offsets the pulse of carbon released during combustion (*9*).

Understanding the net effect of these processes (and their temporal and spatial scales) is important in managing northern forests to mitigate the climate impacts of fossil fuel emissions. Although changes in boreal forest albedo can have a considerable cooling effect on Northern Hemisphere climate (*10*, *11*), these changes are offset by accompanying changes in carbon accumulation (*12*), so the net effect of land cover change on climate may be close to neutral at a global scale when both surface energy balance and CO_2 fluxes are considered (*13*). Here we applied the concept of radiative forcing (*12*) to assess quantitatively the net effect of a boreal forest fire on climate, on the basis of carbon and surface energy budget measurements that we made in a fire chronosequence of black spruce (*Picea mariana*) in interior Alaska. We considered two time scales: the year immediately after fire and an 80-year period during which species composition and ecosystem structure returned to a prefire mature successional state as defined by an adjacent unburned control stand.

The Donnelly Flats crown fire occurred during 11 to 18 June 1999 in interior Alaska (63°55′N; 145°44′W) and burned ~7600 ha (*14*). The fire was intense (e.g., figs. S1 and S2), causing stand-replacing mortality of the black spruce within the burn perimeter and consuming much of the soil organic matter above the mineral horizon (*15*). Aboveground fuel consumption from overstory and understory vegetation was estimated with a combination of harvesting, allometry, and inventory methods. Postfire soil respiration losses during the first year after fire were estimated with a combination of chamber measurements and eddy covariance measurements. Precision spectral pyranometers (Eppley Laboratory, Inc., Newport, RI) measured incoming and outgoing shortwave radiation above the canopy (and thus surface albedo) during July and August of 1999 within the burn perimeter (*7*) and then mostly continuously from October 1999 through September 2004 at both the burn and control.

We converted field measurements of carbon loss during the fire to CH_4 and CO_2 fluxes using emission factors (*16*). Radiative forcing from these greenhouse gases was estimated with equations derived from a global radiative transfer model (*17*). In our figures and table, we report global annual mean radiative forcing (in W) per m^2 of burned area, with radiative forcing defined following the Intergovernmental Panel on Climate Change Third Assessment Report convention as the change in net radiation at the tropopause after stratospheric ad-

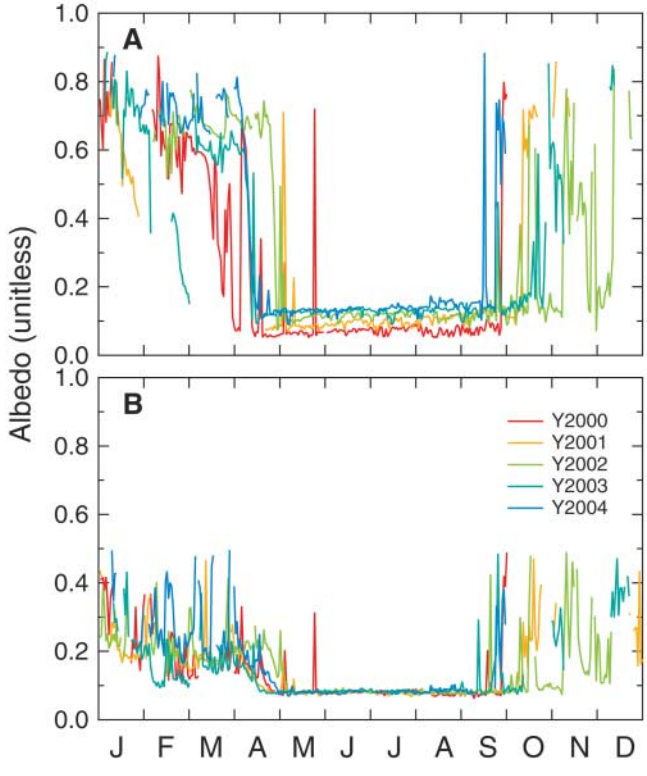

Fig. 1. Midday surface albedo within the burn perimeter of the Donnelly Flats fire (**A**) and from the adjacent black spruce stand that served as a control (**B**). Summer albedo progressively increased during each year and exceeded values at the control site ~3 years after fire. Snow events, including one in late May of 2000, caused spikes that are visible at both the burn and control sites.

[1]Department of Earth System Science, University of California, Irvine, CA 92697, USA. [2]Department of Physics, Atmospheric Science, and General Science, Jackson State University, Jackson, MS 39217, USA. [3]Australian Nuclear Science and Technology Organization, Environmental Division, Menai, NSW 2234, Australia. [4]Atmospheric Chemistry Division, National Center for Atmospheric Research, Boulder, CO 80301, USA. [5]Department of Botany, University of Florida, Gainesville, FL 32611, USA. [6]Environmental Science and Engineering, California Institute of Technology, Pasadena, CA 91125, USA. [7]Institute of Arctic Biology, University of Alaska, Fairbanks, AK 99775, USA. [8]U.S. Geological Survey, Menlo Park, CA 94025, USA. [9]Geological Sciences and Environmental Studies, University of Colorado at Boulder, Boulder, CO 80309, USA.

*To whom correspondence should be addressed. E-mail: jranders@uci.edu

justment (*18*). CH_4 was assumed to have a 10-year atmospheric lifetime. The lifetime of the CO_2 anomaly from the fire was estimated with a combination of ocean impulse-response functions from the Joos and Siegenthaler ocean carbon model (*19*) and a postfire trajectory of net ecosystem production (NEP) that we constructed using mass balance constraints and eddy covariance measurements (figs. S3 and S4). We used the Column Radiation Model (*20*) to estimate radiative forcing from changes in surface albedo within the Donnelly Flats burn perimeter (figs. S5 to S8). The persistence of albedo changes in postfire ecosystems was assessed from an analysis of MODerate Resolution Imaging Spectroradiometer (MODIS) albedo measurements (*21*) within burn perimeters of known ages (*14*) across interior Alaska. We derived radiative forcing from the fire-induced ozone anomaly using simulations from the National Center for Atmospheric Research Community Atmosphere Model version 3 (CAM 3) of the 2004 Alaska and Yukon fire complex (*22*) scaled to the carbon emission levels that we measured for the Donnelly Flats fire. Similarly, we estimated radiative forcing from the direct effect of aerosols and deposition of black carbon on snow and sea ice by injecting emissions from the Donnelly Flats fire into CAM 3 (*23*, *24*). In the Supporting Online Material we provide more information about our methods for estimating radiative forcing, as well as an additional set of forcing estimates that take into account the efficacy of the different agents (*25*).

During the fire event, 206 ± 110 g C m^{-2} were emitted by combustion from the black spruce overstory, 107 ± 74 g C m^{-2} from the vascular plant understory, and 1246 ± 600 g C m^{-2} from the duff layer composed of mosses, lichens, roots, partially decomposed plant litter, and humus. Total fuel consumption for the Donnelly Flats fire (1560 ± 610 g C m^{-2}) was similar to other estimates for boreal North America, including 1580 g C m^{-2} for moderately severe fires in boreal North America (*26*) and 1300 g C m^{-2} for the mean of Canadian boreal forests (*27*). Including additional soil respiration losses of 202 ± 53 g C m^{-2} $year^{-1}$during the first year after fire, the ecosystem lost a total of 1760 ± 620 g C m^{-2}.

Radiative forcing from long-lived greenhouse gases (CH_4 and CO_2) contributed a total of 8 ± 3 W m^{-2} during the first year. Deposition of black carbon on snow and sea ice added another 8 ± 5 W m^{-2}. An increase in tropospheric ozone from fire-emitted trace gases generated a positive radiative forcing of 6 ± 4 W m^{-2}. Fire-emitted aerosols mixed widely across arctic and boreal regions (fig. S9), decreased net radiation at the surface (−90 ± 35 W m^{-2}), but did not substantially change radiative forcing (17 ± 30 W m^{-2}). Changes in surface albedo within the fire perimeter offset positive radiative forcing from the other agents. Specifically, the loss of overstory canopy after fire led to increased snow exposure during spring and fall (fig. S10), higher albedo (Fig. 1), and a negative annual radiative forcing (−5 ± 2 W m^{-2}). The combined effect of all forcing agents was 34 ± 31 W m^{-2} during year 1 (Table 1).

After the first year, the short-lived effects of ozone, aerosols, and black carbon deposition were no longer important, so the net effect of the fire on radiative forcing reflected the balance between the persistence of postfire changes in surface albedo and the effects from the remaining greenhouse gases in the atmosphere. During the first 5 years after fire, summer albedo progressively increased (Fig. 1), probably from an increase in grass and shrub cover and partial loss of black carbon that initially coated soil surfaces and dead black spruce boles. This strengthened the negative radiative forcing from postfire albedo changes, with this quantity decreasing from −5 ± 2 W m^{-2} during the first year to −8 ± 3 W m^{-2} during the period 3 to 5 years after fire. Analysis of MODIS satellite data from nearby forest stands provided evidence that spring and summer albedo typically remains elevated for about three decades after fire and that recovery to prefire albedo levels requires ~55 years (Fig. 2).

We predicted that the greenhouse gas pulse from the Donnelly Flats fire should gradually decline over a period of 5 decades, owing to CH_4 oxidation and CO_2 uptake by the oceans and regrowing vegetation within the burn perimeter (fig. S3D). During this interval, the greenhouse gases will contribute to a positive radiative forcing

Table 1. Radiative forcing associated with the Donnelly Flats fire.

Forcing agent	Radiative forcing* [W (m^2 burned)$^{-1}$]	
	Year 1	Years 0 to 80 (mean)
Long-lived greenhouse gases (CH_4 and CO_2)	8 ± 3	1.6 ± 0.8
Ozone	6 ± 4	0.1 ± 0.1
Black carbon deposition on snow	3 ± 3	0.0 ± 0.0
Black carbon deposition on sea ice	5 ± 4	0.1 ± 0.1
Aerosols (direct radiative forcing)†	17 ± 30	0.2 ± 0.4
Impact at the surface: −90 W ± 35 m^{-2}		
Changes in post-fire surface albedo	−5 ± 2	−4.2 ± 2.0
Total‡	34 ± 31	−2.3 ± 2.2

*All the radiative forcing estimates reported here represent annual mean values (in W) for the global atmosphere associated with burning of a 1-m^2 area within the perimeter of the Donnelly Flats fire. We report values averaged over year 1 and for the mean of the 0- to 80-year period after fire (and including the fire event). †We did not estimate indirect effects of aerosols on radiative forcing as mediated, for example, by cloud drop sizes or cloud lifetime (*4*). Although uncertain, indirect aerosol effects are thought to contribute to negative radiative forcing (*18*, *25*) and would offset other positive radiative forcing agents during year 1. ‡Accounting for the efficacy of the different forcing agents (*25*), the total effective forcing of the Donnelly Flats fire was 18 ± 42 W m^{-2} during year 1 and −2.4 ± 2.3 W m^{-2} during years 0 to 80 (tables S1 and S2).

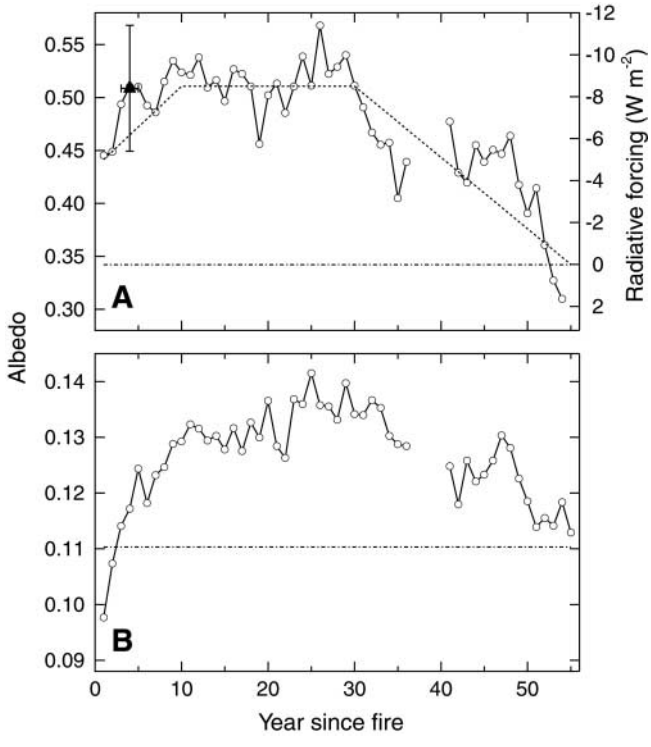

Fig. 2. Postfire albedo during (**A**) spring (Julian Days 33 to 113) and (**B**) summer (Julian Days 145 to 241) from MODIS satellite observations extracted from burn scars of different ages in interior Alaska (circles and solid line, left axis). A control was constructed from the mean of evergreen conifer vegetation that did not burn in the last 55 years (dashed-dotted line, left axis). Annual radiative forcing as estimated from tower measurements of albedo from burn and control sites during 2002 to 2004 was −8 ± 3 W m^{-2} [(A), triangle, right axis]. The longer-term postfire trajectory of albedo-driven annual radiative forcing was assumed to follow the MODIS albedo pattern [(A), dashed line, right axis]. Years with limited burned area were excluded from the analysis.

(Fig. 3A). After ~60 years, continued uptake by the postfire ecosystem should cause atmospheric CO_2 to decrease below background levels, subsequent withdrawal of CO_2 from the ocean, and a negative radiative forcing. As a result of this trajectory and concurrent changes in surface albedo, the influence of the fire on radiative forcing depends on the averaging period (Fig. 3B). Averaged over years 0 to 80, net radiative forcing from the different forcing agents was -2.3 ± 2.2 W m^{-2} (Table 1).

A change in fire return times will have consequences for climate forcing (Fig. 3C), based on the time-since-fire trajectories of the different forcing agents estimated from the Donnelly Flats fire, combined with a stand age model (*28*). If the fire return time decreases [as has been suggested from future warming and drying in continental interiors (*29*)], loss of carbon will increase radiative forcing (Fig. 3C). Accounting for all forcing agents, however, leads to a small negative radiative forcing at the global scale (Fig. 3C) and calls into question the positive feedback that has been suggested in past work. The cooling from a decrease in fire return times is likely to be substantially larger in the Northern Hemisphere, taking into account the spatial pattern of the temperature anomalies resulting from the different forcing agents. Specifically, radiative forcing from greenhouse gases has a widely distributed impact on global temperature (*18*), whereas the influence of postfire changes in surface albedo will be concentrated almost entirely in northern regions (*10*, *11*, *13*, *18*).

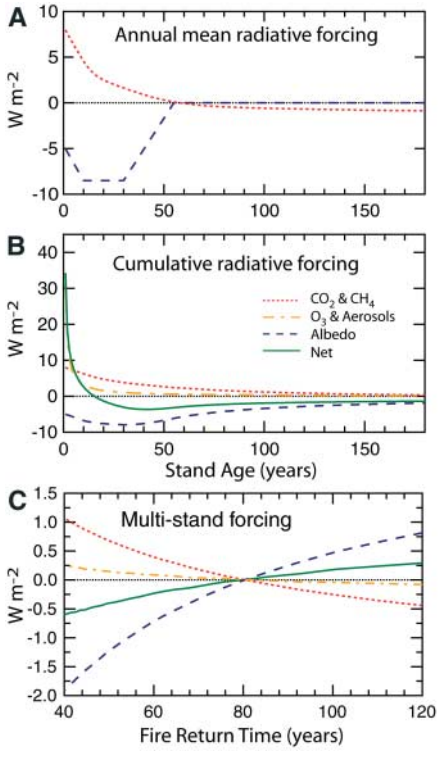

Fig. 3. (**A**) Annual radiative forcing from long-lived greenhouse gases and the postfire trajectory of surface albedo. (**B**) Cumulative annual radiative forcing for the different forcing agents averaged over the time since the fire (or equivalently, the age of the stand). (**C**) Climate forcing of the different components as a function of the fire return time relative to a distribution of stands at steady state with a mean fire return time of 80 years. (C) was constructed with postfire trajectories for the individual agents measured or predicted for the Donnelly Flats fire [e.g., (A)] and the forest stand age distribution model described in the Supporting Online Material. For (C), by definition, each forcing agent had a zero mean at steady state (at a mean fire return time of 80 years).

For the boreal biome as a whole, key factors that are likely to determine the balance between negative and positive radiative forcing associated with fire include burn severity, species establishment in postfire ecosystems, and the duration of winter snow cover. Increased burn severity, for example, may increase aerosol and greenhouse gas emissions, but it is not clear to what extent this may be canceled by greater loss of canopy overstory and consequently higher albedo values during winter and spring. Another unresolved question involves the extent to which fire in Siberian larch forests, which are needleleaf deciduous, has the same influence on postfire surface albedo as reported here for North American needleleaf evergreen forests. Decreases in spring snow cover (*30*) may weaken negative feedbacks associated with postfire increases in surface albedo documented in North America.

Future interactions between the land surface and climate in northern regions may involve both negative feedbacks within the boreal interior (via mechanisms outlined here) and positive feedbacks involving shrub and forest expansion in arctic tundra ecosystems (*31*) and loss of snow cover. Our analysis illustrates how ecosystem processes that generate carbon sources and sinks have inseparable consequences for other forcing agents (*12*, *13*, *32*, *33*). To the extent that the contemporary Northern Hemisphere carbon sink originates from changes in northern forest cover and age (*34*), its value from a climate perspective requires a more nuanced view that encompasses all agents of radiative forcing. Important next steps include reducing uncertainties associated with direct and indirect aerosol effects and disturbance-linked changes in albedo, exploring the combined impacts of feedbacks of the forcing agents estimated here within climate models, and extending this approach to assess the radiative forcing associated with land-cover transitions in temperate and tropical ecosystems.

References and Notes

1. ACIA, "Arctic Climate Impact Assessment" (Cambridge Univ. Press, Cambridge, UK, 2005).
2. W. A. Kurz, M. J. Apps, B. J. Stocks, W. J. A. Volney, in *Biotic Feedbacks in the Global Climate System: Will the Warming Speed the Warming?* G. M. Woodwell, F. Mackenzie, Eds. (Oxford Univ. Press, Oxford, UK, 1995), pp. 119–133.
3. E. S. Kasischke, B. J. Stocks, *Fire, Climate Change, and Carbon Cycling in the Boreal Forest*. M. M. Cadwell *et al.*, Eds., Ecological Studies (Springer, New York, 2000).
4. V. Ramanathan, P. J. Crutzen, J. T. Kiehl, D. Rosenfeld, *Science* **294**, 2119 (2001).
5. S. G. Warren, W. J. Wiscombe, *J. Atmos. Sci.* **37**, 2734 (1980).
6. J. Hansen, L. Nazarenko, *Proc. Natl. Acad. Sci. U.S.A.* **101**, 423 (2004).
7. S. D. Chambers, F. S. Chapin, *J. Geophys. Res.* **108**, 8145 (2002).
8. H. Liu, J. T. Randerson, J. Lindfors, F. S. Chapin, *J. Geophys. Res.* **110**, D13101 (2005).
9. J. W. Harden *et al.*, *Global Change Biol.* **6**, 174 (2000).
10. G. B. Bonan, D. Pollard, S. L. Thompson, *Nature* **359**, 716 (1992).
11. P. K. Snyder, C. Delire, J. A. Foley, *Clim. Dyn.* **23**, 279 (2004).
12. R. A. Betts, *Nature* **408**, 187 (2000).
13. V. Brovkin *et al.*, *Global Change Biol.* **10**, 1253 (2004).
14. The Alaska Fire Service maintains a database of annual fire statistics and geographic information system (GIS) burn perimeters (http://agdc.usgs.gov/data/blm/fire/).
15. J. C. Neff, J. W. Harden, G. Gleixner, *Can. J. For. Res. Rev. Can. Rech. For.* **35**, 2178 (2005).
16. M. O. Andreae, P. Merlet, *Global Biogeochem. Cycles* **15**, 955 (2001).
17. G. Myhre, E. J. Highwood, K. P. Shine, F. Stordal, *Geophys. Res. Lett.* **25**, 2715 (1998).
18. V. Ramaswamy *et al.*, in *Climate Change 2001: The Scientific Basis. Contributions of Working Group 1 to the Third Assessment Report of the Intergovernmental Panel on Climate Change*, J. T. Houghton *et al.*, Eds. (Cambridge Univ. Press, Cambridge, UK, 2001), pp. 350–416.
19. I. G. Enting, T. M. L. Wigley, M. Heimann, "Future Emissions and Concentrations of Carbon Dioxide: Key Ocean/Atmosphere/Land Analyses" (Technical paper no. 31, Commonwealth Scientific and Industrial Research Organization Division of Atmospheric Research, 2001).
20. B. P. Briegleb, *J. Geophy. Res.* **97**, 7603 (1992).
21. C. B. Schaaf *et al.*, *Remote Sens. Environ.* **83**, 135 (2002).
22. G. Pfister *et al.*, *Geophys. Res. Lett.* **32**, L11809 (2005).
23. P. J. Rasch, W. D. Collins, B. E. Eaton, *J. Geophys. Res.* **106**, 7337 (2001).
24. M. G. Flanner, C. S. Zender, *J. Geophys. Res.* **111**, D12208 (2006).
25. J. Hansen *et al.*, *J. Geophys. Res.* **110**, D18104 (2005).
26. E. S. Kasischke *et al.*, *Global Biogeochem. Cycles* **19**, GB1012 (2005).
27. B. D. Amiro *et al.*, *Can. J. For. Res. Rev. Can. Rech. For.* **31**, 512 (2001).
28. E. A. Johnson, *Fire and Vegetation Dynamics: Studies from the North American Boreal Forest*, H. J. B. Birks, Ed., Cambridge Studies in Ecology (Cambridge Univ. Press, Cambridge, UK, 1992).
29. M. D. Flannigan, K. A. Logan, B. D. Amiro, W. R. Skinner, B. J. Stocks, *Clim. Change* **72**, 1 (2005).
30. Z. M. Kuang, Y. L. Yung, *Geophys. Res. Lett.* **27**, 1299 (2000).
31. F. S. Chapin *et al.*, *Science* **310**, 657 (2005).
32. G. P. Robertson, E. A. Paul, R. R. Harwood, *Science* **289**, 1922 (2000).
33. R. A. Pielke *et al.*, *Philos. Trans. R. Soc. London Ser. A* **360**, 1705 (2002).
34. C. L. Goodale *et al.*, *Ecol. Appl.* **12**, 891 (2002).

35. This work was supported by NSF and NASA grants (OPP-0097439 and NNG04GK49G, respectively). We thank M. Prather for advice and C. Dunn, J. Henkelman, J. Raymond, and J. Garron for technical assistance.

Supporting Online Material

www.sciencemag.org/cgi/content/full/314/5802/1130/DC1
Materials and Methods
SOM Text
Figs. S1 to S10
Tables S1 and S2
References and Notes

5 July 2006; accepted 3 October 2006
10.1126/science.1132075